

Capillary Pressure–Saturation Relations for Saprolite: Scaling With and Without Correction for Column Height

E. Perfect,* L. D. McKay, S. C. Cropper, S. G. Driese, G. Kammerer, and J. H. Dane

ABSTRACT

Dense nonaqueous phase liquids (DNAPLs) are important subsurface contaminants. Information is lacking on DNAPL behavior in heterogeneous porous media such as weathered rock (saprolite). We measured air–water and Fluorinert (a nontoxic DNAPL surrogate; 3M, St. Paul, MN)–water capillary pressure–saturation relations, $\theta_w(h_c)$, close to saturation on an 18-cm-long by 10-cm-diameter undisturbed column of interbedded sandstone and clayshale saprolite. The Campbell empirical model was fitted to both $\theta_w(h_c)$ relations. The resulting best-fit parameters were 19.54 and 30.10 cm of H₂O for the displacement capillary pressure head (h_0) and 0.029 and 0.045 for the pore-size distribution index ($1/b$), for the air–water and Fluorinert–water data, respectively. Corresponding model parameters corrected for the hydrostatic fluid distribution within the column were 14.08 and 15.96 cm of H₂O for h_0 , and 0.026 and 0.034 for $1/b$. The correction procedure had a large effect on the Fluorinert–water $\theta_w(h_c)$ relation and relatively little impact on the air–water $\theta_w(h_c)$ relation. Parameters from the air–water relations were used to predict Fluorinert–water $\theta_w(h_c)$ relations using the expression: $(h_0)_2 = (\sigma_2/\sigma_1)(h_0)_1$, where $(h_0)_1$, $(h_0)_2$ and σ_1 , σ_2 are the capillary displacement pressure heads and interfacial tensions with water for air and Fluorinert, respectively. These analyses showed that direct measurements of the Fluorinert–water $\theta_w(h_c)$ relation need to be corrected for column height. The corrected Fluorinert–water $\theta_w(h_c)$ relation was accurately predicted ($R^2 \approx 0.99$) by both the fitted and corrected $(h_0)_1$ values. Thus, the error in prediction introduced by not considering column height or contact angle effects was relatively small. Our results show that scaled air–water $\theta_w(h_c)$ relations can be used to predict DNAPL intrusion into water-saturated saprolite at a physical point.

DENSE NONAQUEOUS PHASE liquids are commonly used as solvents, degreasers, dry cleaning fluids, and pesticide additives. Examples include trichloroethylene, perchloroethene, carbon tetrachloride, chloroform, and polychlorinated biphenyls. As a result of spills, leaks, or intentional releases, DNAPLs are often present in the subsurface environment near industrial plants and waste disposal or storage facilities (Pankow and Cherry, 1996). The need to predict the fate and persistence of these contaminants has stimulated many studies of flow and entrapment of DNAPLs in porous media (see reviews by MacKay et al., 1985; Mercer and Cohen, 1990; Pankow and Cherry, 1996).

Because DNAPL migration and distribution are largely

controlled by capillarity, any attempt to predict DNAPL behavior in a porous medium requires determination of the capillary pressure–saturation relationship, hereafter denoted by $\theta_w(h_c)$, where θ_w is the volumetric content of the wetting fluid and h_c is the capillary pressure head. The standard procedure for measuring $\theta_w(h_c)$ consists of introducing a nonwetting fluid at a known pressure into a porous medium, waiting for an equilibrium condition, and then determining the wetting phase saturation of the sample (Corey, 1994; Lenhard et al., 2002). This procedure produces one pressure–saturation data pair. Additional data pairs are produced by incrementing the nonwetting fluid pressure. The data pairs are then used to construct a static equilibrium drainage curve that describes the capillary behavior of the sample. Such curves are often parameterized using empirical expressions for the $\theta_w(h_c)$ relation such as the Brooks and Corey (1964) equation, the Campbell (1974) equation, and the van Genuchten (1980) equation.

The majority of pressure cell studies involving DNAPL–water systems have been performed on homogeneous porous media (e.g., Lenhard and Parker, 1987; Demond and Roberts, 1991). Relatively little is known about the capillary behavior of DNAPLs in heterogeneous porous media (Kueper et al., 1989; Hinsby et al., 1996; Illangsekare, 1998). The large column sizes required for adequate representation of such materials mean that traditional procedures for measuring the $\theta_w(h_c)$ relation may not be directly applicable.

If the densities of the nonwetting and wetting fluids are different, the capillary pressure will vary with height within the pressure cell (Dane et al., 1992; Liu and Dane, 1995a). Because pressure varies with height, one pressure value cannot represent pressure conditions everywhere within a tall column, but is only representative of one elevation in the sample. Because of this limitation, the standard procedure for measuring capillary behavior suggests that samples should be <2 cm tall. The variation of capillary pressure with height in a sample of this height is negligible in comparison to the relatively large pressures needed to drain the wetting fluid from small pores (Dane and Hopmans, 2002). Thus, little error is introduced by assuming that capillary pressure measured at one elevation within the sample is representative of values throughout the sample.

This height constraint presents a problem for samples containing fractures or macropores. Large undisturbed columns are often needed to obtain a representative sample of the heterogeneity that is present. In these cases, capillary pressure variations with height may be significant in relation to the lower capillary pressures at which

E. Perfect, L.D. McKay, and S.G. Driese, Dep. of Earth and Planetary Sciences, Univ. of Tennessee, Knoxville, TN 37996-1410; S.C. Cropper, 1463 Oxford Place, Cookeville, TN 38506; G. Kammerer, Institute for Hydraulics and Rural Water Management, BOKU, Muthgasse 18, A-1190 Vienna, Austria; J.H. Dane, Dep. of Agronomy and Soils, Auburn Univ., Auburn, AL 36849-5412. Received 19 Jan. 2004. Special Section: Uncertainty in Vadose Zone Flow and Transport Properties. *Corresponding author (eperfect@utk.edu).

Published in Vadose Zone Journal 3:493–501 (2004).
© Soil Science Society of America
677 S. Segoe Rd., Madison, WI 53711 USA

Abbreviations: DNAPL, dense nonaqueous phase liquid; SWSA, Solid Waste Storage Area.

fractures and macropores drain; hence, the height of the sample cannot be neglected.

Additionally, equilibrium saturations within tall columns may not be representative of the entire sample. In a homogeneous material, pores are uniformly distributed throughout the sample, and the displaced fluid comes from all parts of the sample. Thus, the saturation value at any equilibrium step applies to the whole volume of material. In a heterogeneous material, however, the elevation of the interface between immiscible phases within each fracture or macropore will be a function of the aperture size and pressure conditions at each equilibrium step. Thus, it cannot be assumed that the wetting fluid is displaced uniformly from the whole volume of the sample.

Liu and Dane (1995a) developed a computational procedure and a FORTRAN program (Liu and Dane, 1995b) to account for variations of h_c and θ_w with column height. Their approach corrects the parameters of the Brooks and Corey (1964) equation for the height of the experimental column given information on the pressure cell configuration and densities of the wetting and nonwetting fluids. Schroth et al. (1996) used a similar method to correct the parameters of the van Genuchten (1980) equation for column height. More recently, Jalbert and Dane (2001) proposed a correction procedure that does not require a model for the $\theta_w(h_c)$ relation; the method was validated against a simulated data set. Unfortunately, our experience suggests that it is highly sensitive to small fluctuations and does not work well with experimental data. To our knowledge, none of the above methods has been applied to correct the capillary behavior of a DNAPL in a tall column of heterogeneous material. The advantage of such an approach is that once the local parameters are obtained, then the $\theta_w(h_c)$ relation can be up-scaled to any column height of interest.

It is possible to predict DNAPL entry into water saturated voids by scaling the air–water $\theta_w(h_c)$ relation (Leverett, 1941; Parker et al., 1987; Demond and Roberts, 1991). If the capillary displacement pressure head, h_0 , at which an immiscible phase first enters a porous medium is known, then the size of the drained void can be estimated by (Corey, 1994)

$$\ell = \frac{2\sigma \cos \alpha}{h_0 \rho_w g} \quad [1]$$

where ℓ is the pore radius in the case of capillary tube models or the space between two fracture surfaces in the case of parallel plate models, σ is the interfacial tension between the nonwetting and wetting fluid phases, α is the contact angle between the nonwetting fluid and solid phases, ρ_w is the density of water, and g is strength of the gravitational field. It follows that the entry pressure at which another immiscible phase would enter the same material can be predicted from

$$(h_0)_2 = \frac{\sigma_2 \cos \alpha_2}{\sigma_1 \cos \alpha_1} (h_0)_1 \quad [2]$$

where $(h_0)_1$ and $(h_0)_2$ are the displacement pressure heads for Fluids 1 and 2, σ_1 and σ_2 are the interfacial tensions

of Fluids 1 and 2 with water, and α_1 and α_2 are the contact angles with the solid phase for Fluids 1 and 2.

Working with homogeneous porous media, Dumore and Scholls (1974) and Lenhard and Parker (1987) demonstrated that the $\theta_w(h_c)$ relation of one immiscible fluid can be scaled by the ratio of interfacial tensions to give a good approximation of relations for other immiscible fluids in the same material. This implies that α does not change significantly and that for equivalent saturations, the capillary pressure relation between two different immiscible fluids in the same material can be approximated by

$$(h_0)_2 \approx \frac{\sigma_2}{\sigma_1} (h_0)_1 \quad [3]$$

Equation [3] suggests that the capillary behavior of a hazardous DNAPL such as trichloroethylene can be predicted from the measured capillary behavior of a non-hazardous immiscible fluid such as air. This approach does not appear to have been tested on a heterogeneous porous medium. Moreover, since Eq. [3] is based on h_0 , it is likely that not correcting for column height will have a significant impact on the accuracy of the scaling procedure in the case of such materials.

The objectives of this study were to (i) experimentally determine capillary pressure–saturation relations for DNAPL and air intrusion into an initially water-saturated heterogeneous porous medium, (ii) correct these relations for finite column height effects, (iii) evaluate the impact of this correction on the prediction of the DNAPL–water $\theta_w(h_c)$ relation from the air–water $\theta_w(h_c)$ relation, and (iv) compare pore-size distributions inferred from the capillary pressure–saturation relations with those observed in thin section.

MATERIALS AND METHODS

Column Excavation and Preparation

The heterogeneous porous medium used in this study was saprolite (isovolumetrically weathered and decomposed bedrock) excavated from a research site in Solid Waste Storage Area 7 (SWSA 7) on the Oak Ridge Reservation in eastern Tennessee, USA. The SWSA 7 location was chosen because it is well characterized and the saprolite is soft enough to be easily excavated with hand tools (Driese et al., 2001). The saprolite retains bedding features and fracture characteristics of the underlying unweathered sandstone and clayshale parent rocks. There are three distinct fracture sets; one set occurs along the bedding planes, while two sets cut across bedding (Dreier et al., 1987; Cumbie, 1997). Previous hydrologic investigations have demonstrated the major role these fractures play in flow and transport at this site (Wilson et al., 1989, 1992; Jardine et al., 1993; Cumbie, 1997; Driese et al., 2001; McKay et al., 2002).

A column of saprolite (≈ 10 cm in diameter) was excavated in the field using procedures developed by Jardine et al. (1993) and Cumbie (1997) to minimize sample disturbance. The column was carved so its long axis was oriented parallel to both bedding (which dipped at 69° to the southeast) and the in situ subsurface water flow direction. Bedding strike was N34E. The sample was excavated from a depth of 90 to 108 cm below ground surface.

In the laboratory, the saprolite sample was trimmed to fit inside an 18-cm-long, 10-cm-diameter PVC casing. Epoxy was

Table 1. Physical properties of fluids used in the different experiments (3M Specialty Materials, 1999).

Fluid	Property†		
	Density	Dynamic viscosity	Interfacial tension‡
	g cm^{-3}	Pa s^{-1}	mN m^{-1}
Air	0.0	2×10^{-5}	72
Fluorinert	1.9	4×10^{-3}	52
Water	1.0	9×10^{-4}	–

† At standard temperature and pressure.

‡ Relative to water.

then poured into the annulus to prevent fluid flow between the sample and casing, and end caps with influent and effluent connections were attached. Trimmings from the column were used to estimate bulk density (ρ_b) using the clod method (Grossman and Reinsch, 2002). Total porosity (ϕ) was calculated from ρ_b assuming a particle density of 2.67 g cm^{-3} as described by Flint and Flint (2002).

After assembly the column was saturated with degassed 0.005 M CaCl_2 solution. This solution (hereafter referred to as water) was used as the saturation fluid throughout the study. It was chosen to minimize dispersion of pedogenic clays within the sample. The saturation fluid was applied to the bottom of the column by raising the applied head in 1- to 2-cm increments for several days to minimize air entrapment. The saturated hydraulic conductivity (K_{sat}) was measured using the steady-state flow method after complete saturation was achieved (Dane et al., 2002).

Before conducting the capillary pressure–saturation experiments, the effluent end cap was temporarily removed and a water-saturated porous ceramic plate, with an air-entry value of 500 cm, was placed in direct contact with the sample and firmly attached with epoxy. After reassembly, the column was flushed with water. The completed pressure cell did not leak when tested at pressure heads of up to 290 cm.

Capillary Pressure–Saturation Measurements

Air was the first immiscible fluid introduced into the pressure cell. After that experiment the column was slowly rewetted with water to bring the sample back to complete saturation. The second immiscible fluid introduced was Fluorinert FC-40, a clear, colorless, multipurpose, nonhazardous perfluorocarbon (3M Specialty Materials, 1999). Fluorinert was employed as a surrogate DNAPL because of its physical similarity to common hazardous contaminants such as perchloroethene. Selected physical properties of the fluids used are given in Table 1.

Pressure cell configurations for the air–water and Fluorinert–water capillary pressure–saturation experiments are illustrated in Fig. 1. The drainage behavior of the sample was determined by injecting the nonwetting fluid at the influent end of the column, with pressure controlled by a digital screw pump (GDS Instruments, Hook, Hampshire, UK). The pressure controller could maintain injection head targets set by the operator in the range of 0 to 1000 cm of H_2O . The control transducer could resolve head changes to 0.1 cm, and head targets could be in increments as small as 0.25 cm.

Incrementing the applied pressure raised the nonwetting fluid pressure in the cell because the nonwetting fluid could not exit the column through the ceramic capillary barrier. This increase in nonwetting pressure created a temporary total pressure gradient in the column. In response to this imposed gradient, the wetting fluid passed through the capillary barrier and through the effluent tubing into a collection flask until equilibrium was regained. In this way, the nonwetting fluid pressure was incremented while the wetting fluid pressure stayed constant, controlled by the elevation where the effluent tubing was open to the atmosphere. Data collected during drainage are in the form of a nonwetting pressure (expressed as cm of H_2O) at the influent end of the sample, $P_n(z_n)$, the volume of water displaced from the sample through the effluent line, and the volume of nonwetting phase injected by the pressure controller. The time allowed for equilibrium to be established for each pressure increment was judged by the operator from continuously displayed information on volume and pressure change reported by the data logging equipment.

Because air is less dense than water, it was injected from the top of the column (i.e., $z_n = 17.9 \text{ cm}$). The effluent tubing was open to the atmosphere at an elevation of $z_w = 18.6 \text{ cm}$, so the pressure head of the wetting fluid at this elevation, $P_w(z_w)$, was constant at 0 cm (Fig. 1). During air injection, 84 pressure targets were set over a head range of 0 to 220 cm. The average target increment was 2 cm, and equilibrium times varied from a few minutes up to 21 h. The air injection experiment lasted 13 d.

Fluorinert was injected from the bottom of the column because it is denser than water (i.e., $z_n = 0 \text{ cm}$). The pressure cell was inverted so the flow direction was the same as during the air injection (Fig. 1). The effluent tubing was open to the atmosphere at an elevation of $z_w = 18.25 \text{ cm}$, so $P_w(z_w)$ was constant at 0 cm. A total of 153 pressure targets were set during the Fluorinert injection. The average target increment was 1.4 cm, and equilibrium times varied from a few minutes to 184 h. The Fluorinert injection experiment lasted 54 d.

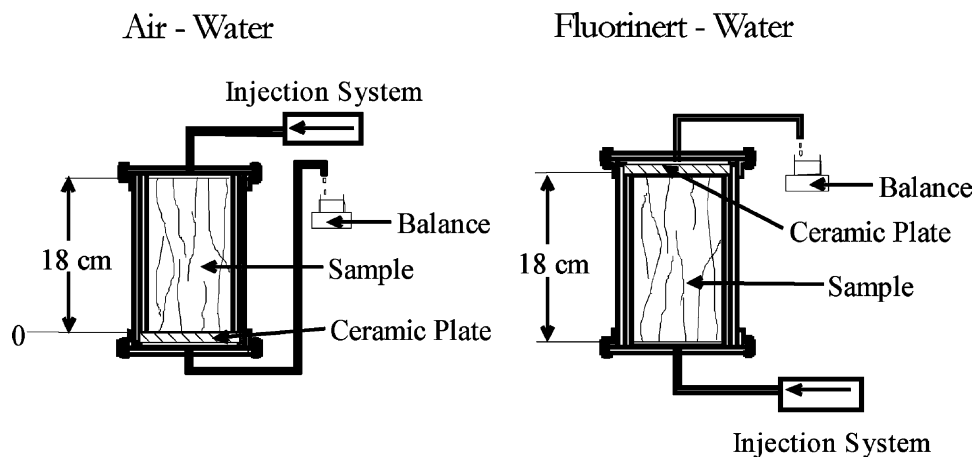


Fig. 1. Pressure cell configurations for the air–water and Fluorinert–water experiments.

Saprolite Petrography

After the capillary–pressure saturation experiments were completed, the column was dismantled, and hand specimens approximately 2.5 cm thick were sawed from both the inlet and outlet ends and allowed to completely air dry. These samples were first coated and impregnated with Hillquist (Fall City, WA) epoxy while heated on a hot plate, then cut (while dry) with a diamond trim saw into 5 by 8 cm diameter billets, and finally polished to 600 grit using wet–dry industrial sandpaper. The billets were glued to large-format commercial glass slides with Hillquist epoxy, and after 24 to 48 h were cut off (while dry) with a diamond trim saw to about 3- to 5-mm thickness. Thin sections were prepared (while dry) to standard optical thickness (30 μm) using progressively finer grades of sandpaper, as described in Mora et al. (1993). Quartz has a first-order gray interference color in thin sections that are prepared to this thickness. Micromorphological analysis was conducted using standard geological and soil petrographic techniques (Brewer, 1976; Pettijohn et al., 1987; FitzPatrick, 1993).

Data Analysis and Scaling

The capillary pressure head at the influent level, h_c , was calculated using the expression (Liu and Dane, 1995a):

$$h_c = \frac{P_n(z_n) - P_w(z_w)}{\rho_w g} \quad [4]$$

where $P_w(z_w)$ is the wetting fluid pressure measured at elevation z_w , and $P_n(z_n)$ is non-wetting fluid pressure measured at elevation z_n . For the air–water experiment, the average volumetric water content of the saprolite, $\bar{\theta}_w$, was calculated from ϕ and the measured volume of water displaced from the sample during each pressure increment. For the Fluorinert–water experiment, $\bar{\theta}_w$ was calculated from ϕ and the measured volume of Fluorinert injected into the sample. The volume of Fluorinert injected was used in place of the volume of water displaced because a power interruption caused a partial loss of data for the volume of water displaced. Because Fluorinert is virtually incompressible and insoluble in water, the volume of Fluorinert injected was assumed to approximate the volume of water that was displaced. Capillary pressure–saturation relations were then constructed by plotting $\bar{\theta}_w$ vs. h_c .

The $\bar{\theta}_w(h_c)$ relations were parameterized using the Campbell (1974) empirical model:

$$\bar{\theta}_w = \phi \left(\frac{h_0}{h_c} \right)^{1/b} \quad h_c > h_0 \quad [5a]$$

$$\bar{\theta}_w = \phi \quad h_c \leq h_0 \quad [5b]$$

where h_0 is the displacement capillary pressure head and $1/b$ is the pore-size distribution index. Equation [5] was given preference over other empirical models for the capillary pressure–saturation relation because it has the same form as physically based expressions for the drainage of mass fractals (Tyler and Wheatcraft, 1990; Giménez et al., 1997). It is equivalent to the Brooks and Corey (1964) expression when the residual saturation parameter in that model is zero.

Equation [5] was fitted to the $\bar{\theta}_w$ vs. h_c data using segmented nonlinear regression analysis based on the Newton iterative procedure (SAS Institute, 1997). The h_0 and $1/b$ parameters were treated as fitted values, while ϕ was fixed to be the measured value. Convergence was achieved for both fits according to the SAS Institute (1997) default criterion. Best estimates of the Campbell (1974) parameters obtained in this manner are referred to hereafter as fitted values.

In the capillary pressure–saturation relations determined

Table 2. Pressure cell configurations for the different experiments.

Parameter†	Experiment	
	Air–water‡	Fluorinert–water§
z_c , cm	17.90	17.90
z_n , cm	17.90	0.00
z_w , cm	18.60	18.25

† As defined in Lui and Dane (1995a, 1995b).

‡ Air injected at top of column.

§ Fluorinert injected at bottom of column.

above, h_c corresponds to a specific elevation, whereas $\bar{\theta}_w$ is an average value for the entire column. Multiphase fluids in heterogeneous porous media often produce nonuniform distributions of h_c and θ_w in a column of finite height (Dane et al., 1992). Thus, the fitted Campbell (1974) parameters may not represent the true behavior of the porous medium at a physical point. Liu and Dane (1995a) showed that the local θ_w is related to the average $\bar{\theta}_w$ by

$$\bar{\theta}_w = \frac{1}{z_c} \int_0^{z_c} \theta_w(h_c) dz \quad [6]$$

Inserting Eq. [5] into Eq. [6] and performing the integration yields three analytical expressions relating $\bar{\theta}_w$ to θ_w for the conditions: $\rho_w = \rho_n$, $\rho_w < \rho_n$, and $\rho_w > \rho_n$, where ρ_n is the density of the nonwetting fluid. For a given pressure cell geometry and fluid density pair, the unknown parameters in these expressions are the point estimates of h_0 and $1/b$. Thus, by fitting the analytical expressions for $\bar{\theta}_w(h_c)$ to the measured capillary pressure–saturation relationship, best estimates of the local Campbell (1974) parameters can be obtained. We used TrueCell (Jalbert et al., 1999), a Windows interface based on the Liu and Dane (1995b) Fortran program, to perform this fitting procedure. Input values for the fluid densities and pressure cell characteristics used in TrueCell are given in Tables 1 and 2, respectively. The ϕ was fixed to be the measured value, and since TrueCell is based on the Brooks and Corey (1964) equation, residual saturation was set to zero. Best estimates of h_0 and $1/b$ obtained in this manner are referred to hereafter as corrected values.

The corrected and fitted Campbell (1974) parameters from the air–water experiment were used to predict the fitted and corrected Fluorinert–water capillary pressure–saturation relations using Eq. [3]. In this study 1 in Eq. [3] denotes air while 2 denotes Fluorinert; therefore from Table 1, $\sigma_2/\sigma_1 = 0.72$.

RESULTS AND DISCUSSION

Micromorphological analysis of thin sections indicated that about 80 to 90% of the saprolite was fine-grained (modal size estimated as between 0.06 and 0.08 mm in diameter), parallel- to ripple cross-laminated, glauconitic quartz arenite to glauconitic subarkose arenite (classification of McBride, 1963). Monocrystalline quartz with straight to undulatory extinction constituted about 80% of the framework grains, whereas about 5% of the grains were finely polycrystalline quartz (chert), 10% of the detrital grains were twinned potassium feldspars, and about 4% of detrital grains were glauconite. The sandstone lithology occurred in beds ranging from 0.5 to 5 cm in thickness. Detrital phyllosilicate grains (chiefly muscovite and biotite) and heavy mineral grains (primarily zircon, tourmaline, and ilmenite) constituted about 1% of the framework grain population. Quartz grains ranged from subangular to subrounded, and were well sorted. Millimeter-thick cross-laminae exhibited normal

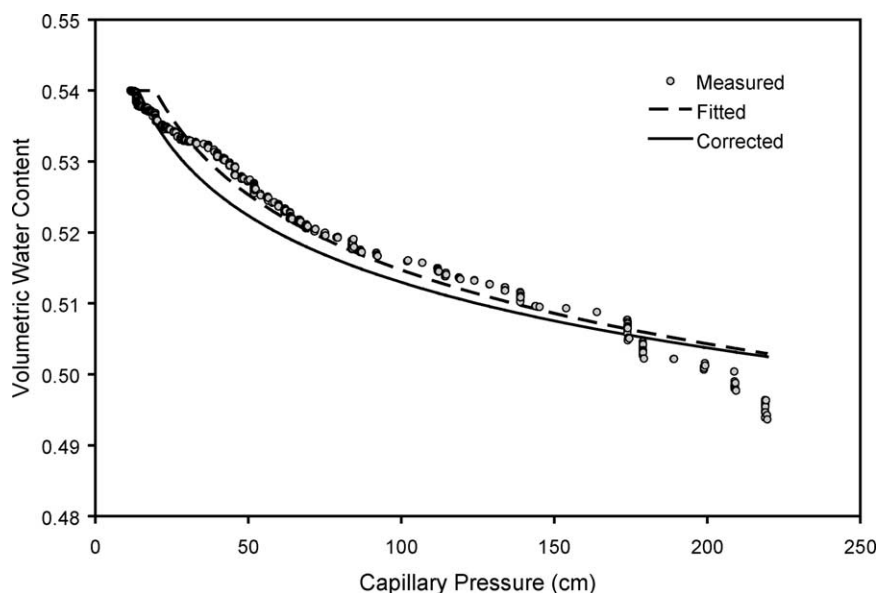


Fig. 2. Measured capillary pressure–saturation data for the air–water experiment along with fitted and corrected Campbell (1974) relations.

size grading that ranged from fine silt (top of laminae) to very fine sand (base of laminae).

The remaining 10 to 20% of the saprolite consisted of horizontally bedded and bedding-perpendicular clayshale layers and lenses that varied from 0.05 to 2 mm in thickness. Depositional clayshale (i.e., originally deposited as part of the parent material) was a characteristic greenish-gray color and showed some evidence of ductile flow related to tectonic deformation of the bedrock. Pedogenic clays constituted 10 to 15% of the saprolite and appeared distinctly different from the depositional clayshale. They were reddish-colored in transmitted light, and exhibited a strong birefringence fabric in cross-polarized light.

A continuous distribution of void sizes was present, consisting of root pores, partially infilled fractures, and matrix pores in both the sandstone and clayshale beds. Each thin section contained between one and three fresh root pores (filled with undecayed root tissue) that ranged from 0.5 to 2 mm in diameter, plus partially to completely clay-filled old root pores. All of the root pores were circular and occurred in clay-rich seams, often bedding-parallel fractures infilled with pedogenic clay.

The fractures were geometrically complex and were partially to completely infilled with pedogenic clays. Bedding-parallel fractures typically followed primary depositional clay layers; these fractures ranged from 0.05 to 1.5 mm wide, as judged from the thickness of pedogenic clay infillings. Orthogonal bedding-perpendicular fractures typically cross-cut the sandstone beds at very high angles (60–90° with respect to bedding orientation). These fractures ranged from 0.05 to 1 mm wide, although most were <0.3 mm wide, as judged from the thickness of pedogenic clay infillings, and were spaced between 0.3 and 1.5 cm apart. The amount of open fracture porosity (i.e., unoccluded by pedogenic clay) was impossible to quantify from the thin sections, because nearly all of the clay infillings experienced desiccation-induced shrinkage to varying degrees. The

sandstone beds contained relatively large matrix pores while those in the clayshale layers were much smaller. Variations in the amount of infilling of the sandstone matrix, fracture network, and old root pores probably contributed to the wide range of voids present.

The total porosity (ϕ) of the column was $0.54 \text{ m}^3 \text{ m}^{-3}$. This value is consistent with previous investigations of the saprolite at the SWSA 7 site, which report $0.39 \leq \phi \leq 0.55$ (Wilson et al., 1992; Jardine et al., 1993; Cumbie, 1997; Driese et al., 2001). Despite the high ϕ , the saturated hydraulic conductivity (K_{sat}) of the column was only $4.0 \times 10^{-6} \text{ m s}^{-1}$, probably due to partial blockage of pores and fractures by pedogenic clays. This value falls within the range of previously measured K_{sat} values for saprolite at this site, which are summarized in Fig. 2 of Driese et al. (2001).

Measured capillary pressure–saturation relationships for the air and Fluorinert intrusion experiments are shown in Fig. 2 and 3, respectively. The data are plotted as the capillary pressure head calculated at the sample influent level as a function of the volumetric water content. Both $\bar{\theta}_w(h_c)$ relations were similar. Once the displacement pressure head was exceeded, the pore volume invaded increased gradually, confirming the wide range of pore sizes observed in the thin sections. There was no evidence of rapid drainage from the fracture network and root pores. There are at least two possible explanations for this behavior. First, it is possible that fracture drainage was impeded by the presence of the pedogenic clay infillings. Thus, drainage from matrix pores would be hard to distinguish from fracture drainage. Alternatively, because there was a distribution of capillary pressures with height within the column, fracture drainage could have occurred from parts of the sample even when other parts of the fracture network had ceased draining. The most likely explanation is some combination of both effects.

The Campbell (1974) model fitted the observed capillary pressure–saturation relations reasonably well. The

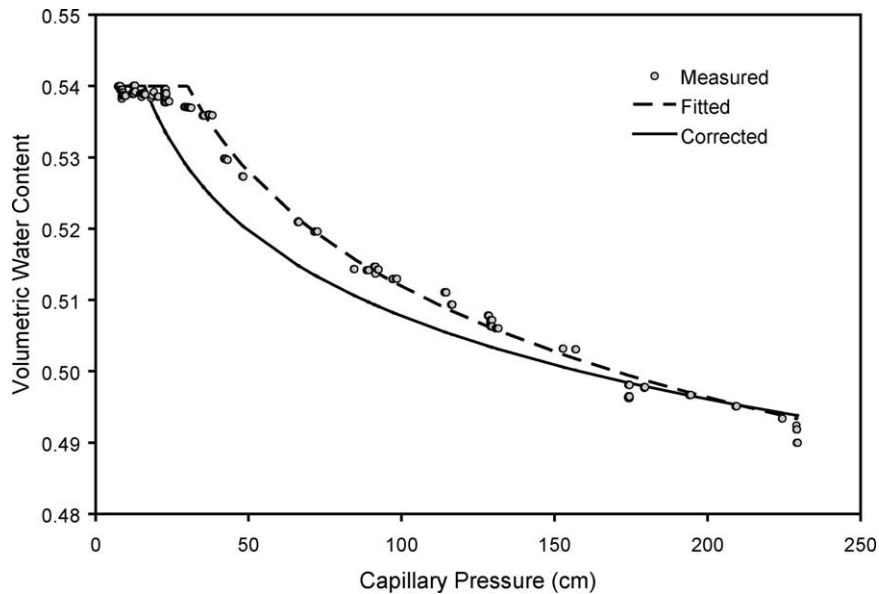


Fig. 3. Measured capillary pressure–saturation data for the Fluorinert–water experiment along with fitted and corrected Campbell (1974) relations.

residual sums of squares for the two fits were 0.013 and 0.004 for the air–water and Fluorinert–water data sets, respectively. The resulting parameter estimates are summarized in Table 3. The $1/b$ values, which should be independent of the non-wetting fluid used, were quite dissimilar ($\Delta = 36\%$), indicating a significant effect of column height on the estimated pore-size distribution index. The predicted curves from these fits are shown in Fig. 2 and 3. The Campbell (1974) model normally produces a sharp displacement entry pressure at a physical point. Thus, close to saturation there is some discrepancy between the observed and predicted values of $\bar{\theta}_w$ in both experiments (Fig. 2 and 3). Model predictions also deviated somewhat from the observed $\bar{\theta}_w$ values at $h_c > 175$ cm in the air intrusion experiment (Fig. 2). The reasons for this discrepancy are unclear, but the fact that the Fluorinert intrusion data did not show a similar trend suggests it was not related to drainage of a distinct fracture or pore domain.

Correcting the Campbell (1974) equation fits for the hydrostatic fluid distribution within the column resulted in significant changes to both model parameters (Table 3). After correction the $1/b$ values for the air–water and Fluorinert–water experiments were much closer ($\Delta = 24\%$), as they should be. Moreover, based on Eq. [1] with $\alpha = 0$ and $\rho_w = 1 \text{ g cm}^{-3}$, the corrected h_0 values yielded more consistent estimates of the maximum fracture width (ℓ) than the fitted values. Results for the fitted h_0 values were $75 \mu\text{m}$ for air intrusion and $35 \mu\text{m}$ for Fluorinert intrusion, a discrepancy of $\Delta = 53\%$. In

contrast, the difference between the maximum fracture widths based on the corrected h_0 values ($\ell = 104$ and $66 \mu\text{m}$ for the air–water and Fluorinert–water data sets, respectively) was only $\Delta = 37\%$. The improved equivalencies obtained for the corrected $1/b$ and ℓ values as compared with the fitted values demonstrate the value of Liu and Dane's (1995a) computational procedure.

The mass fractal dimension (D), a physically based geometric measure of the range of void sizes present, was calculated from the corrected $1/b$ values using the expression (Giménez et al., 1997):

$$D = 3 - \frac{1}{b} \quad [7]$$

For both the air–water and Fluorinert–water data sets, $D \approx 2.97$. The fact that D is so close to three indicates a medium dominated by small pores and a slow drainage regime. We are unaware of any previous estimates of D for saprolite. However, comparison of our result with D values for different textured soils (Brakensiek and Rawls, 1992) suggests that the void-size distribution in this material is analogous to that of clay. Thus, the thin interbedded clayshale layers and pedogenic clay infillings appear to dominate the hydrologic properties of the saprolite even though it was derived mainly from sandstone.

Predicted capillary pressure–saturation relations based on the corrected Campbell (1974) model parameters in Table 3 are included in Fig. 2 and 3. Except for a slight decrease in the displacement capillary pressure head, the correction procedure had relatively little impact on the overall form of the air–water relation. In contrast, there were major changes to the form of the Fluorinert–water relation: the displacement pressure head was almost halved, and the slope of the drainage curve was reduced (Fig. 3).

To evaluate the potential for predicting DNAPL intrusion into water-saturated saprolite based on air intru-

Table 3. Fitted and corrected Campbell (1974) parameters† for the different experiments.

Experiment	Procedure	h_0	$1/b$
Air–water	fitted	19.54	0.029
	corrected	14.08	0.026
Fluorinert–water	fitted	30.10	0.045
	corrected	15.96	0.034

† As defined in Eq. [5].

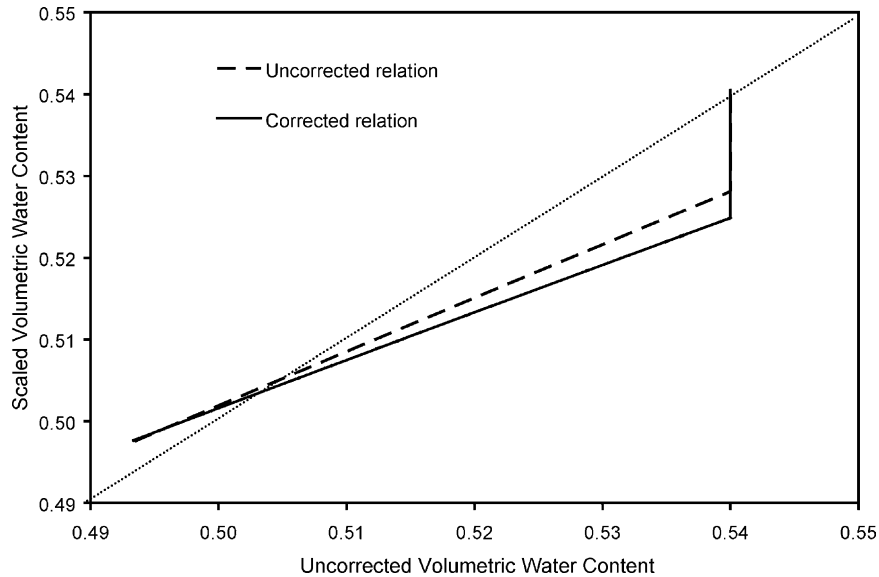


Fig. 4. Scaled volumetric water contents from the fitted and corrected air–water relations vs. volumetric water contents from the fitted Fluorinert–water relation.

sion data, scaled volumetric water contents were calculated from the Campbell (1974) air–water parameters using Eq. [3] and compared with those obtained from the Fluorinert–water experiment (Fig. 4 and 5). The scaling procedure was unable to reproduce the fitted Fluorinert–water relation; the predictions underestimated high values of θ_w and overestimated lower values (Fig. 4). In contrast, both the fitted and corrected scaled air–water parameters resulted in approximately 1:1 regression lines (intercept = 0.05, slope = 0.90 and intercept = 0.08, slope = 0.84 for the fitted and corrected predictions, respectively) that explained approximately 99% of the total variation in the corrected Fluorinert–water relation (Fig. 5).

The above results demonstrate the influence of column height on the Fluorinert–water experiment, as well as the lack of sensitivity of the air–water data to this ef-

fect. These different responses can be attributed to the density differences between air and Fluorinert. The accuracy of the scaling procedure was only revealed after correction of the Fluorinert intrusion data for height effects. In contrast, correction of the air–water data did not appear to be a prerequisite for accurate scaling. This is because the saprolite behaved much like a clay soil, and as Liu and Dane (1995a) pointed out, the correction procedure is most useful for coarse materials.

Contact angles were not measured for the fluid pairs used in this study. Demond and Roberts (1991) showed that such measurements can improve scaling of capillary pressure–saturation relations in the case of homogeneous porous media. However, Fig. 5 suggests that the error introduced by assuming $\alpha_a = \alpha_b = 0$ in Eq. [2] was negligible for the more heterogeneous material used in this study.

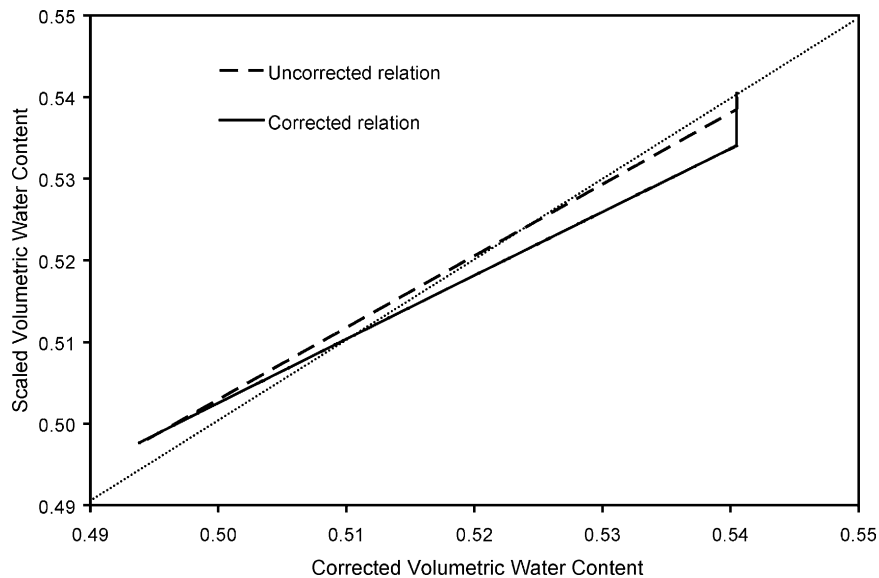


Fig. 5. Scaled volumetric water contents from the fitted and corrected air–water relations versus volumetric water contents from the corrected Fluorinert–water relation.

CONCLUSIONS

Micromorphological analyses of thin sections and capillary pressure-saturation relations indicated that sandstone-clayshale saprolite at the SWSA 7 site has a continuous distribution of void sizes. One of the principal causes of this distribution is the variable infilling of fracture apertures, and root and sandstone matrix pores, with pedogenic clays.

The Campbell (1974) equation provided a good fit to the measured air-water and Fluorinert-water capillary pressure-saturation relations. Our results indicate that for DNAPL-water systems the parameters of this model are very sensitive to the hydrostatic fluid distribution within a tall column and require correction for this effect. Failure to do so can result in significant overestimation of the displacement pressure, which determines if a nonwetting fluid will enter a finer layer or not.

From a practical perspective our most significant result is the demonstration that air intrusion measurements can be successfully employed, in conjunction with Eq. [3], to predict DNAPL entry into a water-saturated heterogeneous porous medium at a physical point. Under the conditions of this study, the magnitude of the error introduced by not correcting the air-water parameters used in the scaling procedure for column height effects or differences in contact angle was relatively small.

REFERENCES

- 3M Specialty Materials. 1999. Fluorinert electronic liquids for electronic reliability testing: Application information. 3M Specialty Materials, St. Paul, MN.
- Brakensiek, D.L., and W.J. Rawls. 1992. Comment on "Fractal processes in soil water retention" by Scott W. Tyler and Stephen W. Wheatcraft. *Wat. Resour. Res.* 28:601-602.
- Brewer, R. 1976. *Fabric and mineral analysis of soils*. R.E. Krieger Publishing, New York.
- Brooks, R.H., and A.T. Corey. 1964. Hydraulic properties of porous media. *Hydrology Paper 3*. Colorado State University, Fort Collins.
- Campbell, G.S. 1974. A simple method for determining unsaturated conductivity from moisture retention data. *Soil Sci.* 117:311-314.
- Corey, A.T. 1994. *Mechanics of immiscible fluids in porous media*. 3rd ed. Water Resources Publications, Highlands Ranch, CO.
- Cumbie, D.H. 1997. Laboratory scale investigations into the influence of particle diameter on colloid transport in highly weathered shale saprolite. M.S. thesis. Department of Geological Sciences, University of Tennessee, Knoxville.
- Dane, J.H., and J.W. Hopmans. 2002. Hanging water column. p. 680-684. *In* J.H. Dane and G.C. Topp (ed.) *Methods of soil analysis*. Part 4. SSSA Book Ser. 5. SSSA, Madison, WI.
- Dane, J.H., R.J. Lenhard, and M. Oostrom. 2002. Relative permeability measurements. p. 1581-1590. *In* J.H. Dane and G.C. Topp (ed.) *Methods of soil analysis*. Part 4. SSSA Book Ser. 5. SSSA, Madison, WI.
- Dane, J.H., M. Oostrom, and B.C. Missildine. 1992. An improved method for the determination of capillary pressure-saturation curves involving TCE, water and air. *J. Contam. Hydrol.* 11:69-81.
- Demond, A.H., and P.V. Roberts. 1991. Effect of interfacial forces on two-phase capillary pressure-saturation relationships. *Water Resour. Res.* 27:423-437.
- Dreier, R.B., D.K. Soloman, and C.M. Beaudoin. 1987. Fracture characterization in the unsaturated zone of shallow land burial facility. p. 51-59. *In* D. D. Evans and T. J. Nicholson (ed.) *Flow and transport through unsaturated fractured rock*. Geophysical Monogr. 42. AGU, Washington, DC.
- Driese, S.G., L.D. McKay, and C.P. Penfield. 2001. Lithologic and pedogenic influences on porosity distribution and groundwater flow in fractured sedimentary saprolite: A new application of environmental sedimentology. *J. Sediment. Res.* 71:843-857.
- Dumore, J.M., and R.S. Scholls. 1974. Drainage capillary pressure functions and the influence of connate water. *SPE J.* 14:437-444.
- Fitzpatrick, E.A. 1993. *Soil microscopy and micromorphology*. John Wiley and Sons, New York.
- Flint, L.E., and A.L. Flint. 2002. Porosity. p. 241-254. *In* J.H. Dane and G.C. Topp (ed.) *Methods of soil analysis*. Part 4. SSSA Book Ser. 5. SSSA, Madison, WI.
- Giménez, D., E. Perfect, W.J. Rawls, and Y. Pachepsky. 1997. Fractal models for predicting soil hydraulic properties: A review. *Eng. Geol.* 48:161-183.
- Grossman, R.B., and T.G. Reinsch. 2002. Bulk density and linear extensibility. p. 201-228. *In* J.H. Dane and G.C. Topp (ed.) *Methods of soil analysis*. Part 4. SSSA Book Ser. 5. SSSA, Madison, WI.
- Hinsby, K., L.D. McKay, P. Jørgensen, M. Lenczewski, and C.P. Gerba. 1996. Fracture aperture measurements and migration of solutes, viruses and immiscible creosote in a column of clay-rich till. *Ground Water* 34:1065-1075.
- Illangasekare, T.H. 1998. Flow and entrapment of nonaqueous phase liquids in heterogeneous soil formations. p. 417-435 *In* H. Magdi-Selim and L. Ma (ed.) *Physical nonequilibrium in soil: Modeling and application*. Ann Arbor Press, Chelsea, MI.
- Jalbert, M., and J.H. Dane. 2001. Correcting laboratory retention curves for hydrostatic fluid distributions. *Soil Sci. Soc. Am. J.* 65: 648-654.
- Jalbert, M., J.H. Dane, and J.H. Liu. 1999. TrueCell: Physical point Brooks-Corey parameters using pressure cell data, Users guide for version 1.2. Department of Agronomy and Soils, Special Rep. Alabama Agric. Exp. Stn., Auburn University, Auburn, AL.
- Jardine, P.M., G.K. Jacobs, and G.V. Wilson. 1993. Unsaturated transport processes in undisturbed heterogeneous porous media: I. Inorganic contaminants. *Soil Sci. Soc. Am. J.* 57:945-953.
- Kueper, B.H., W. Abbot, and G. Farquhar. 1989. Experimental observations of multiphase flow in heterogeneous media. *J. Contam. Hydrol.* 5:83-95.
- Lenhard, R.J., J.H. Dane, and M. Oostrom. 2002. Saturation-pressure relationships. p. 1565-1579. *In* J.H. Dane and G.C. Topp (ed.) *Methods of soil analysis*. Part 4. SSSA Book Ser. 5. SSSA, Madison, WI.
- Lenhard, R.J., and J.C. Parker. 1987. Measurement and prediction of saturation-pressure relationships in three-phase porous media systems. *J. Contam. Hydrol.* 1:407-424.
- Leverett, M.C. 1941. Capillary behavior in porous solids. *Trans. Soc. Pet. Eng. AIME* 142:152-169.
- Liu, H.H., and J.H. Dane. 1995a. Improved computational procedure for retention relations of immiscible fluids using pressure cells. *Soil Sci. Soc. Am. J.* 59:1520-1524.
- Liu, H.H., and J.H. Dane. 1995b. Computation of the Brooks-Corey parameters at a physical point based on pressure cell data. Department of Agronomy and Soils, Special Rep. Alabama Agric. Exp. Stn., Auburn University, Auburn, AL.
- MacKay, D.M., P.V. Roberts, and J.A. Cherry. 1985. Transport of organic contaminants in groundwater: Distribution and fate of chemicals in sand and gravel aquifers. *Environ. Sci. Technol.* 19: 384-392.
- McBride, E.F. 1963. A classification of common sandstones. *J. Sediment. Petrol.* 33:664-669.
- McKay, L.D., A.D. Harton, and G.V. Wilson. 2002. Influence of flow rate on transport of bacteriophage in shale saprolite. *J. Environ. Qual.* 31:1095-1105.
- Mercer, J.W., and R.M. Cohen. 1990. A review of immiscible fluids in the subsurface: Properties, models, characterization and remediation. *J. Contam. Hydrol.* 6:107-163.
- Mora, C.I., D.E. Fastovsky, and S.G. Driese. 1993. *Geochemistry and Stable Isotopes of Paleosols: A short course manual for the Annual Meeting of the Geological Society of America Convention*. Studies in Geology 23. Dep. Geol. Sci., University of Tennessee, Knoxville.
- Pankow, J.F., and J.A. Cherry. 1996. *Dense chlorinated solvents and other DNAPL's in groundwater*. Waterloo Press, Portland, OR.
- Parker, J.C., R.J. Lenhard, and T. Kuppasamy. 1987. A parametric model for constitutive properties governing multiphase flow in porous media. *Water Resour. Res.* 23:618-624.

- Pettijohn, F.J., P.E. Potter, and R. Siever. 1987. Sand and sandstone. 2nd ed. Springer-Verlag, New York.
- SAS Institute Inc. 1997. SAS/STAT Software: Changes and enhancements through release 6.12 ed. SAS Inst., Cary, NY.
- Schroth, M.H., S.J. Ahearn, J.S. Selker, and J.D. Istok. 1996. Characterization of Miller-similar silica sands for laboratory subsurface hydrologic studies. *Soil Sci. Soc. Am. J.* 60:1331–1339.
- Tyler, S., and S.W. Wheatcraft. 1990. Fractal processes in soil water retention. *Water Resour. Res.* 26:1047–1054.
- van Genuchten, M.Th. 1980. A closed-form equation for predicting the hydraulic conductivity of unsaturated soils. *Soil Sci. Soc. Am. J.* 44:892–898.
- Wilson, G.V., J.M. Alfonsi, and P.M. Jardine. 1989. Spatial variability of saturated hydraulic conductivity of the subsoil of two forested watersheds. *Soil Sci. Soc. Am. J.* 53:679–685.
- Wilson, G.V., P.M. Jardine, and J.P. Gwo. 1992. Modeling the hydraulic properties of a multiregion soil. *Soil Sci. Soc. Am. J.* 56:1731–1737.